Plant Reproduction (2018) 31:89–105
https://doi.org/10.1007/s00497-017-0315-0

ORIGINAL ARTICLE

Regulation of floral meristem activity through the interaction of *AGAMOUS*, *SUPERMAN*, and *CLAVATA3* in *Arabidopsis*

Akira Uemura[1] · Nobutoshi Yamaguchi[1,2] · Yifeng Xu[3] · WanYi Wee[3] · Yasunori Ichihashi[2,4] · Takamasa Suzuki[5] · Arisa Shibata[4] · Ken Shirasu[4,6] · Toshiro Ito[1]

Received: 29 August 2017 / Accepted: 28 November 2017 / Published online: 7 December 2017

Key message **Floral meristem size is redundantly controlled by *CLAVATA3*, *AGAMOUS*, and *SUPERMAN* in *Arabidopsis*.**

Abstract The proper regulation of floral meristem activity is key to the formation of optimally sized flowers with a fixed number of organs. In *Arabidopsis thaliana*, multiple regulators determine this activity. A small secreted peptide, CLAVATA3 (CLV3), functions as an important negative regulator of stem cell activity. Two transcription factors, AGAMOUS (AG) and SUPERMAN (SUP), act in different pathways to regulate the termination of floral meristem activity. Previous research has not addressed the genetic interactions among these three genes. Here, we quantified the floral developmental stage-specific phenotypic consequences of combining mutations of *AG, SUP,* and *CLV3*. Our detailed phenotypic and genetic analyses revealed that these three genes act in partially redundant pathways to coordinately modulate floral meristem sizes in a spatial and temporal manner. Analyses of the *ag sup clv3* triple mutant, which developed a mass of undifferentiated cells in its flowers, allowed us to identify downstream targets of AG with roles in reproductive development and in the termination of floral meristem activity. Our study highlights the role of AG in repressing genes that are expressed in organ initial cells to control floral meristem activity.

Keywords *Arabidopsis thaliana* · Floral meristem · CLAVATA3 · AGAMOUS · SUPERMAN · Reproductive development

Introduction

Organ development in plants mainly occurs post-embryonically, with both external and internal inputs influencing the final shapes of the organs. Meristems possess a small self-maintaining group of pluripotent stem cells that give rise to all organs. These stem cells are located in the central zone of a dome-shaped meristem. Cells in the peripheral zone of the meristem divide faster than those in the central zone and become organ initial cells, also known as founder cells (Chandler 2011). The balance between cell proliferation and differentiation in these two functional zones is determined as a result of the integration of external and internal inputs. After the integration, interactions of multiple factors are thought to act as developmental outputs.

Communicated by Tetsuya Higashiyama.

Nobutoshi Yamaguchi and Yifeng Xu have contributed equally to this work.

Electronic supplementary material The online version of this article (https://doi.org/10.1007/s00497-017-0315-0) contains supplementary material, which is available to authorized users.

✉ Toshiro Ito
itot@bs.naist.jp

[1] Biological Sciences, Nara Institute of Science and Technology, 8916-5, Takayama, Ikoma, Nara 630-0192, Japan

[2] Precursory Research for Embryonic Science and Technology, Japan Science and Technology Agency, 4-1-8, Honcho, Kawaguchi-shi, Saitama 332-0012, Japan

[3] Temasek Life Sciences Laboratory, 1 Research Link, National University of Singapore, Singapore 117604, Republic of Singapore

[4] RIKEN Center for Sustainable Resource Science, 1-7-22 Suehiro, Tsurumi, Yokohama, Kanagawa 230-0045, Japan

[5] Department of Biological Chemistry, College of Bioscience and Biotechnology, Chubu University, 1200 Matsumoto-cho, Kasugai, Aichi 487-8501, Japan

[6] Graduate School of Science, The University of Tokyo, Bunkyo, Tokyo 113-0033, Japan

Flower development depends on the presence of determinate floral meristems. Floral meristem activity is necessary to produce floral organ primordia, but the meristematic activity must be fully terminated after sufficient cell proliferation has occurred (Sun and Ito 2015). In *Arabidopsis thaliana*, a key determinant gene for floral meristem establishment is *WUSCHEL* (*WUS*), which encodes a homeodomain protein (Laux et al. 1996; Mayer et al. 1998). WUS activity is precisely controlled at both the transcriptional and translational levels (Perales et al. 2016; Rodriguez et al. 2016), and mutations in this gene cause striking defects in the floral meristems; for example, *wus-1* flowers lack carpels (Laux et al. 1996). WUS acts as both an activator and a repressor of gene expression (Ikeda et al. 2009) by interacting with various partners. In addition to forming a transcriptional repression complex with TOPLESS and HISTONE DEACETYLASE19 (Kieffer et al. 2006; Szemenyei et al. 2008), or with HAIRY MERISTEM (Zhou et al. 2015), WUS provides a different function. The stability of the WUS protein is maintained by DNA-dependent homodimerization (Rodriguez et al. 2016).

Multiple regulators of *WUS* mRNA levels have been identified. The *WUS* mRNA expression domain is largely restricted to the organizing center located below the shoot and floral meristems, which is necessary to maintain the stem cell population (Laux et al. 1996). A negative feedback loop controlled by a CLAVATA (CLV) signaling pathway governs stem cell homeostasis. The CLV pathway determines the level of *WUS* expression and prevents the accumulation of excess stem cells (Fletcher et al. 1999; Brand et al. 2000; Schoof et al. 2000; Kondo et al. 2006; Gruel et al. 2016). A leucine-rich repeat receptor kinase, CLV1, and a secreted peptide, CLV3, function as a ligand–receptor pair (Ogawa et al. 2008). *CLV3* is expressed in the stem cell domain of floral meristems (Fletcher et al. 1999). WUS directly binds to a group of tightly clustered *cis*-elements in the *CLV3* promoter to control its transcription (Perales et al. 2016), while the CLV3 signaling pathway in turn negatively regulates *WUS* expression. Mutants of *CLV3* possess enlarged floral meristems and have higher levels of *WUS* expression due to the absence of this negative feedback loop (Clark et al. 1995; Brand et al. 2000; Szczesny et al. 2009).

Another negative feedback loop functions to terminate stem cell activity during flower development (Doerner 2001). The floral determinacy regulator gene *AGAMOUS* (*AG*) is synergistically activated by WUS and the floral meristem identity regulator LEAFY (LFY), beginning at stage 3 of flower development (Smyth et al. 1990; Yanofsky et al. 1990; Weigel et al. 1992; Lenhard et al. 2001; Lohmann et al. 2001). AG controls many reproductive developmental processes by activating or repressing its ~ 2000 direct targets (Ito et al. 2004, 2007; Gomez-Mena et al. 2005; Sun et al. 2009; Liu et al. 2011; Ó'Maoiléidigh et al. 2013). AG is required for determinacy; termination of floral meristem activity is delayed in flowers of the *ag* mutant, which results in flowers within flowers (Yanofsky et al. 1990). In certain conditions, such as short-day photoperiods or treatments with gibberellic acid, *ag* flowers show an inflorescence-like reversion (Okamuro et al. 1996). AG both directly and indirectly represses *WUS* expression through the precise control of histone modifications, and fully inhibits *WUS* expression during stage 6 of floral development (Sun et al. 2009, 2014; Liu et al. 2011). Another regulator of *WUS* expression in flowers is the transcriptional repressor SUPERMAN (SUP), which contains a C_2H_2 zinc-finger DNA-binding domain and an EAR repression domain (Bowman et al. 1992; Sakai et al. 1995). Since *SUP* is expressed in the cells surrounding the floral meristem at stage 3, the effect of SUP on *WUS* expression is largely non-cell-autonomous (Ito et al. 2003; Prunet et al. 2017).

The genetic interactions between the *AG* and *SUP,* the *AG* and *CLV* and the *SUP* and *CLV* pathways have previously been examined (Bowman et al. 1992; Meyerowitz 1997; Breuil-Broyer et al. 2016). Bowman et al. (1992) revealed that *ag sup* double mutants indeterminately produce additional whorls of petals from undifferentiated cells, while Meyerowitz (1997) reported that *ag clv1* double mutants have an excessive number of organs and whorls. Breuil-Broyer et al. (2016) showed that *sup* alleles crossed to the *clv1* resulted in synergistic enhancement of stamen number increase and carpelloidy. These findings suggest that these signaling pathways are largely distinct in their control of meristematic cell proliferation and differentiation in floral development; however, previous research has not investigated the potential genetic interactions among *AG*, *SUP*, and *CLV3*.

To further understand the coordinated actions of AG, SUP, and CLV3 in controlling the determination of the floral meristem, we generated double and triple mutants of these three genes and quantitatively analyzed their meristematic phenotypes. Our analysis revealed specific spatial and temporal roles for CLV3, AG, and SUP in floral meristem determinacy, enabling a coordinated modulation of floral meristem sizes in parallel pathways. Furthermore, an RNA-seq analysis was conducted to compare the transcriptomes of floral buds from the *ag sup clv3* triple mutant with those of the double mutant with functional AG activity (*sup clv3*), enabling the systematic identification of genes and processes that depend on AG function in the floral meristem. Our findings suggest that AG functions to maintain the irreversible state of reproductive development through the negative regulation of floral meristem identity genes and genes involved in organ initiation.

Materials and methods

Genetic stocks and growth conditions

This study used the *A. thaliana* mutants *ag-1*, *clv3-2*, and *sup-1*, and *pWUS::GFP-ER* lines, all of which were in the

Landsberg *erecta* genetic background, and which have all been described previously (Bowman et al. 1989, 1992; Clark et al. 1995; Gordon et al. 2007). The double and triple mutants were generated by genetic crosses and were identified in the F2 or later generations using PCR genotyping. Primer sequences are provided in Supplementary Table 1. Mutants containing transgenes were identified in the F2 or later generations by selection with antibiotics and PCR genotyping. All plants were grown on soil under continuous light conditions at 22 °C.

Phenotypic and statistical analyses

To quantify the size of flowers, at least 20 flower images were taken from the wild type, single, double, and triple mutants, respectively, for analyses. To minimize the environmental differences in growth chambers, these plants were grown side-by-side at the same density in each pot. Images for each genotype at stage 13, when buds open (Smyth et al. 1990) were quantified by Image J (NIH). Student's *t* test was conducted to evaluate the statistical significance.

SEM

Scanning electron microscopy (SEM) was performed as previously described (Yamaguchi and Komeda 2013), with minor modifications. Prior to floral tissue fixation, flowers older than stage 10 were removed with forceps. The floral tissues were fixed overnight in a solution containing 45% ethanol, 5% formaldehyde, and 5% acetic acid, then dehydrated through an ethanol and acetone series. The resulting tissues were critical-dried with liquid CO_2 using a critical point dryer (EM CPD300; Leica Microsystems) and coated with gold using an E-1010 sputter coater (Hitachi) before SEM imaging. The tissues were imaged under an S-4700 SEM (Hitachi) with an accelerating voltage of 15 kV. More than five floral primordia for each genotype were observed.

Tissue sectioning

Sectioning was performed as previously described (Yamaguchi and Komeda 2013), with minor modifications. To minimize the environmental differences in the growth chambers, the plants used for sectioning were grown side-by-side at the same density in each pot. Flowers older than stage 8 were removed with forceps, and the remaining floral tissues were fixed overnight in 45% ethanol, 5% formaldehyde, and 5% acetic acid, and then dehydrated through a series of ethanol solutions. The 100% ethanol was replaced using a Technovit 7100 resin solution (Heraeus), and the floral tissues were incubated at room temperature overnight. The resin-containing tissues were then polymerized, and 10-μm longitudinal sections were made using a RM2255 microtome (Leica Microsystems). The sections were placed onto a microscope slide and stained with 0.05% toluidine blue (Wako Chemicals) and then observed under an Axio Scope A1 microscope (Carl Zeiss). From serial sections in the abaxial–adaxial axis, floral primordia or floral buds cutting in the centers were selected for the height and width measurements. The height and width of the floral meristems were determined from at least 13 floral primordia or floral buds from individual plants of each genotype. Images for each genotype at specific developmental stages were quantified in ImageJ (National Institutes of Health). A Student's *t* test was conducted to evaluate the statistical significance of the data.

GFP observation

Confocal microscopy was performed as previously described (Yamaguchi et al. 2016), with minor modifications. After using forceps to remove flowers older than stage 8, the inflorescences were embedded into a 5% agar block. A Liner Slicer PRO7 vibratome (Dosaka) was used to obtain 35-μm sections, which were placed onto a microscope slide in a drop of water, covered with a cover glass, and observed under a confocal laser scanning microscope (FV1000: Olympus) with a UPlanSApo objective lens (Olympus). More than five floral buds at each floral stage were observed for each genotype.

RNA-seq

An RNeasy Plant Mini Kit (Qiagen) was used to extract total RNA from four biological replicates of *sup-1 clv3-2* and *ag-1 sup-1 clv3-2* floral buds up to stage 10 of flower development. DNA was removed using an RNase-Free DNase Set (Qiagen), and the mRNA was extracted from the total RNA using oligo-dT magnetic beads (New England Biolabs). An RNA library was prepared using the Breath Adapter Directional sequencing method for strand-specific 3′ Digital Gene Expression (Townsley et al. 2015). Briefly, the mRNA was fragmented using magnesium ions at elevated temperatures, after which the polyA tails of mRNA were primed using an adapter-containing oligonucleotide for cDNA synthesis with DNA Polymerase I (Thermo Fisher Scientific). The 5′ adapter addition was performed using breath capture to generate strand-specific libraries. The final PCR enrichment was performed using oligonucleotides containing the full adapter sequence with different indexes and Phusion High-Fidelity DNA Polymerase (New England Biolabs). The cleanup and size selection of the resulting cDNA was performed using AMPure XP beads (Beckman Coulter). The size distribution and concentration of the library were measured using agarose gel electrophoresis and a microplate photometer, respectively, to enable the pooling of libraries for Illumina

sequencing systems. The libraries were sequenced by NextSeq 500 (Illumina). The produced bcl files were converted to fastq files by bcl2fastq (Illumina). The data were deposited into the DNA Data Bank of Japan (DRA006355).

Data analysis

AG ChIP-seq data, organ-initial-cell transcriptomic data, and floral-organ-specific transcriptomic data were obtained from Ó'Maoiléidigh et al. (2013), Frerichs et al. (2016), and Jiao and Meyerowitz (2010), respectively. Genes of interest were identified and characterized as previously described (Winter et al. 2015), with minor modifications. An overlap between differentially expressed genes in *sup clv3* and *ag sup clv3* and the AG-bound genes was examined and visualized using VENNY 2.1 (http://bioinfogp.cnb.csic.es/tools/venny/index.html). To examine the overlap of the two datasets, a Chi-square test was performed in R (https://www.r-project.org/). A gene ontology (GO) term enrichment analysis was conducted using the agriGO web-based tool and database (http://bioinfo.cau.edu.cn/agriGO/). The TreeMap view of GO terms and interactive graph view were generated with REVIGO (http://revigo.irb.hr/) after minimizing redundant enriched GO terms. MeV (http://mev.tm4.org/#/welcome) was used to generate a heatmap and perform k-mean clustering.

RT-PCR

RT-PCR was performed as previously described (Yamaguchi et al. 2014, 2017), with minor modifications. RNA was extracted using an RNeasy Plant Mini Kit (Qiagen). To minimize contamination by genomic DNA, an RNase-Free DNase Set (Qiagen) was used prior to cDNA synthesis, which was performed using a PrimeScript 1st strand cDNA Synthesis Kit (Takara). The resulting cDNA was quantified with a LightCycler 480 (Roche) using FastStart Essential DNA Green Master mix (Roche). The results of the RT-PCR experiments were normalized against the internal control gene, *EIF4* (*At3g13920*). Two independent experiments were performed, and similar results were obtained. The RT-PCR primers are listed in Supplementary Table 1.

Results

Characterization of single, double, and triple mutant flowers of *ag-1*, *sup-1*, and *clv3-2*

Prior to our detailed genetic interaction assay of *AG*, *SUP*, and *CLV3*, we first confirmed the previously reported phenotypes of the single and double mutants. A wild-type *Arabidopsis* flower consists of four types of organ: four sepals, four petals, six stamens, and two carpels (Fig. 1a). Since AG controls the termination of floral meristem activity and the identity of the floral organs, the *ag-1* flowers had more whorls of organs in a repeating sepal–petal–petal sequence (Fig. 1b; Bowman et al. 1989; Yanofsky et al. 1990). The *sup-1* flowers produced approximately ten stamens, but had fewer, smaller carpels than the wild type (Fig. 1c; Bowman et al. 1992; Sakai et al. 1995). Although the numbers of its floral organs varied, the *clv3-2* flowers often had increased numbers in each of the four whorls (Fig. 1d; Clark et al. 1995; Fletcher et al. 1999). The flowers of the single mutants were slightly larger than those of the wild type because of the increased numbers of whorls and/or organs (Fig. 1a–d) (WT vs. *ag-1*: $p = 4.1 \times 10^{-11}$, WT vs. *sup-1*: $p = 1.3 \times 10^{-8}$, WT vs. *clv3-2*: 2.7×10^{-9}). As previously reported (Bowman et al. 1992), *ag-1 sup-1* forms numerous whorls of petals after a single whorl of sepals (Fig. 1e), resulting in larger flowers than those of the single mutants (*ag-1* vs. *ag-1 sup-1*: $p = 1.5 \times 10^{-8}$). At the center of the *ag-1 sup-1* flowers is a mass of undifferentiated cells (Fig. 1f).

To understand the genetic interactions between *AG* and *CLV3* in flower development, we generated the *ag-1 clv3-2* double mutant. As reported for the *ag-1 clv1* double mutant (Meyerowitz 1997), *ag-1 clv3-2* had increased numbers of organs and whorls, as well as larger flowers, compared with those of the single mutants (Fig. 1b, d, g) (*ag-1* vs. *ag-1 clv3-2*: $p = 8.3 \times 10^{-12}$). In *ag-1 clv3-2*, numerous sepals and petals were produced around a mass of undifferentiated meristematic cells (Fig. 1h), which appeared to be much larger than that of the *ag-1 sup-1* flowers (Fig. 1f, h).

To examine the effect of mutations in both *SUP* and *CLV3*, we generated the *sup-1 clv3-2* double mutant. The *sup-1 clv3-2* flowers had a *clv3-2*-like phenotype in terms of sepal and petal number (Fig. 1d, i). As reported in *sup-1 clv1-6* (Breuil-Broyer et al. 2016), *sup-1 clv3-2* exhibited an increased number of stamens compared with the parental lines (Fig. 1i, j), and the size of the stigmatic region of *sup-1 clv3-2* at the tip of the gynoecium was larger than that of the *clv3-2* single mutant (Fig. 1d, i, j); a mass of undifferentiated cells was surrounded by an enlarged stigma-like structure. Because the organ number defects were enhanced in the double mutant, the size of the flowers of *sup-1 clv3-2* was slightly increased (*clv3-2* vs. *sup-1 clv3-2*: $p = 8.1 \times 10^{-5}$).

To further investigate the genetic interactions among *CLV3*, *AG*, and *SUP*, we generated triple mutants. The *ag-1 sup-1 clv3-2* triple mutant had a large increase in the numbers of petal whorls produced after a single whorl of sepals, which was much more pronounced than those of the single mutants or either double mutant combination (Fig. 1a–l) (*ag-1 clv3-2* vs. *ag-1 sup-1 clv3-2*: $p = 7.2 \times 10^{-6}$). The region of undifferentiated cells in the center of the triple mutant flowers was similar to that of *ag-1 clv3-2* (Fig. 1f, h, j, k).

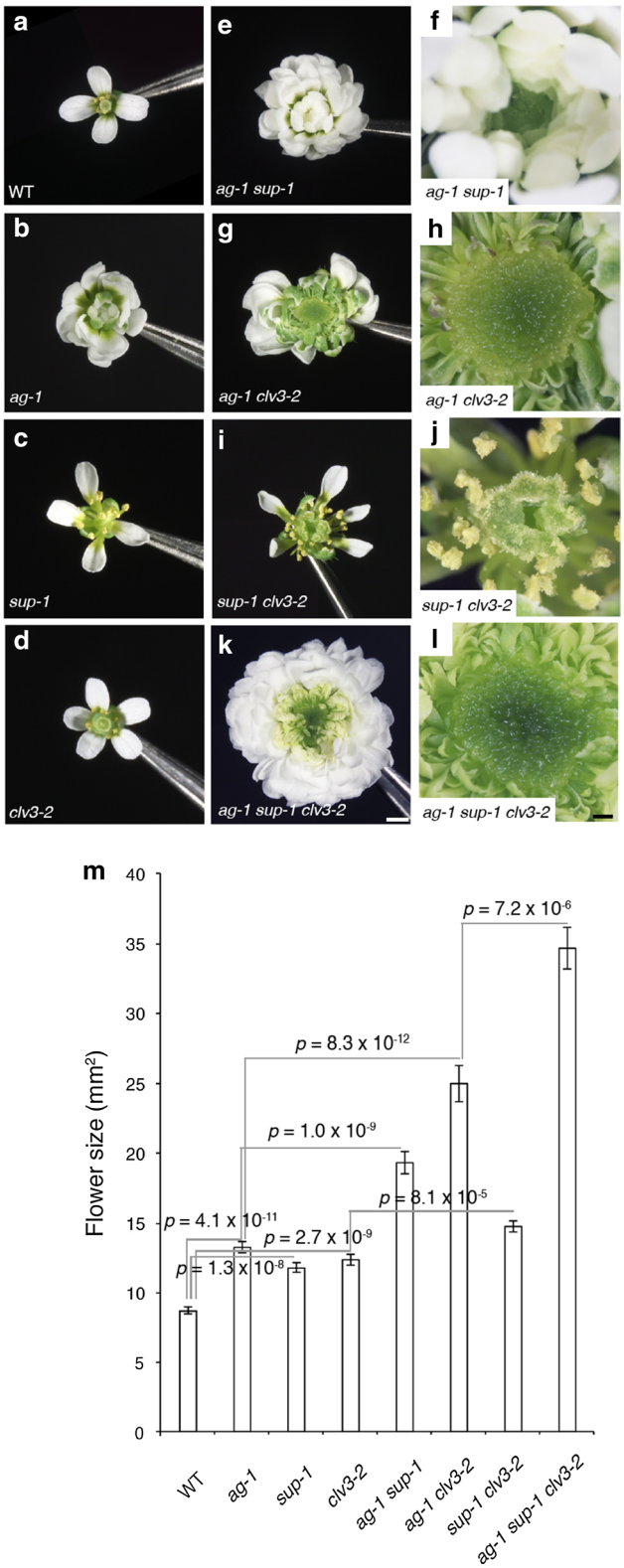

Fig. 1 Comparison of flower size between the wild type and single, ▶ double, and triple mutants. **a**–**l** Top views of the flowers formed in wild type (**a**), *ag-1* (**b**), *sup-1* (**c**), *clv3-2* (**d**), *ag-1 sup-1* (**e**, **f**) *ag-1 clv3-2* (**g**, **h**), *sup-1 clv3-2* (**i**, **j**), and *ag-1 sup-1 clv3-2* (**k**, **l**). **f**, **h**, **j**, **l** A mass of undifferentiated cells located in the center of some mutant flowers is shown. **m** Quantification of flower size. Error bars represent SD of at least 13 measurements. The *p* values were calculated using a Student's *t* test. Bar = 1 mm in **a**–**e**, **g**, **i**, and **k**; 200 µm in **f**, **h**, **j**, and **l**

Sizes of the mutant floral meristems at floral developmental stage 3

Changes in the size of flowers and/or the number of floral organs are often correlated with the height and width of the floral meristems (Clark et al. 1995; Laux et al. 1996; Sawa et al. 1999). We quantified the heights and widths of floral meristems at stage 3 of flower development using SEM and sectioning in the adaxial–abaxial axis (Fig. 2a–i). No significant difference was observed in the heights (from the groove between sepal primordia and inner parts to the top of the floral meristem) and the widths (between the two grooves along the lateral axis) of floral meristems between the wild type, *ag-1,* and *sup-1* at stage 3 of flower development ($p > 0.01$; Fig. 2a–c, i, j). As previously reported (Clark et al. 1995), approximately 1.5-fold and 1.1-fold increases in the heights and widths of *clv3-2* stage 3 floral meristems were observed relative to the wild type, respectively; both *clv3-2* values were significantly greater than those of the wild type ($p = 2.9 \times 10^{-8}$ and $p = 1.9 \times 10^{-5}$), *ag-1*, and *sup-1* (Fig. 2d, i, j).

We next characterized the heights and widths of the floral meristems in the double and triple mutants. No significant difference in height or width was observed between the *ag-1 sup-1* double mutant and its parental lines ($p > 0.01$), nor did a mutation in the *AG* gene alter the *clv3-2* phenotype of the stage 3 meristems ($p > 0.01$; Fig. 2b, c, e, i, j). By contrast, the *sup-1* mutation had a statistically significant effect in the sensitized *clv3* mutant background at stage 3, enhancing the defect in floral meristem height observed in *clv3* ($p = 2.2 \times 10^{-3}$), but not in the meristem width ($p > 0.01$). The average heights of stage 3 floral meristems in *clv3-2* and *sup-1 clv3-2* were about 25 and 31 µm, respectively. In the *ag-1 sup-1 clv3-2* triple mutant, the width of the floral meristems at stage 3 was similar to those of *clv3-2*, *ag-1 clv3-2*, and *sup-1 clv3-2* (Fig. 2d, f–h, j). By contrast, the floral meristems of *ag-1 sup-1 clv3-2* were taller than those of any of the parental lines (Fig. 2g–i), with a statistically significant difference between the floral meristem heights of *ag-1 sup-1 clv3-2* and *sup-1 clv3-2*, which had the tallest floral meristems among the double mutants ($p = 2.3 \times 10^{-3}$).

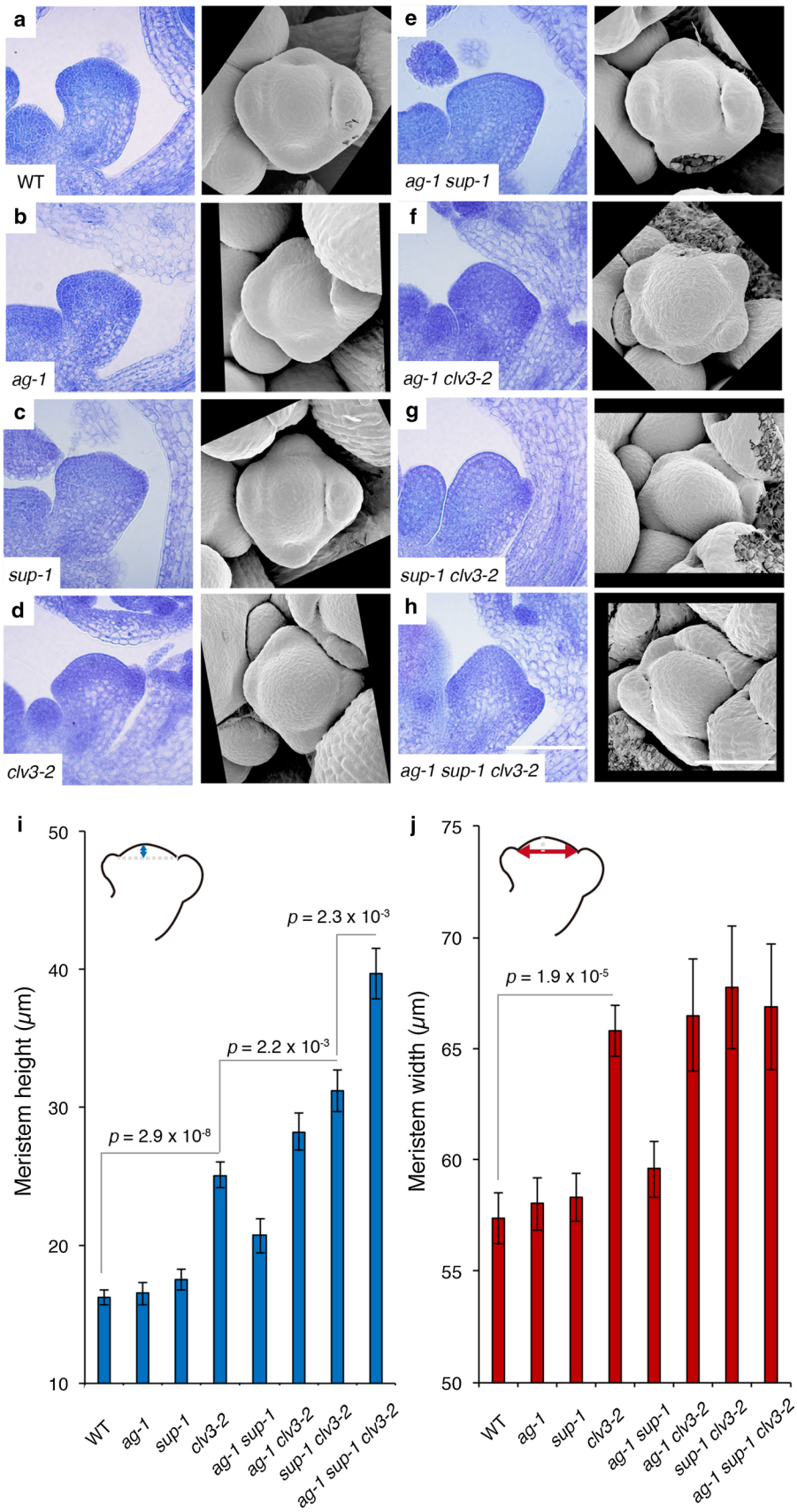

Fig. 2 Comparison of floral meristem height and width between the wild type and single, double, and triple mutant floral buds at stage 3. **a**–**h** Side and top views of the floral buds at stage 3 formed in wild type (**a**), *ag-1* (**b**), *sup-1* (**c**), *clv3-2* (**d**) *ag-1 sup-1* (**e**) *ag-1 clv3-2* (**f**), *sup-1 clv3-2* (**g**), and *ag-1 sup-1 clv3-2* (**h**). (Left) Side views from longitudinal sections. (Right) Top views visualized using SEM. Section and SEM images are shown at the same magnification. Bar = 50 µm in **a**–**h**. **i**, **j** Quantification of floral meristem height (**i**) and width (**j**) in floral buds at stage 3. Error bars represent SD of at least 13 measurements. The *p* values were calculated using a Student's *t* test

Sizes of the mutant floral meristems at floral developmental stage 5

To further address the roles of *AG*, *SUP*, and *CLV3* in floral meristem proliferation, floral meristems at stage 5 were characterized in detail (Fig. 3a–j). There was no difference in the heights and widths of the floral meristems between the wild type and *ag-1* ($p > 0.01$), suggesting that the increased size of the *ag-1* flowers mainly occurs after stage 5 (Fig. 3a, b, i, j). In the *sup-1* mutant, an increase in floral meristem width ($p = 6.6 \times 10^{-4}$) relative to the wild type becomes apparent by stage 5 (Fig. 3a, c, i, j). The average floral meristem height and width of *clv3-2* were significantly higher those of the wild type ($p = 1.2 \times 10^{-14}$ and $p = 1.5 \times 10^{-4}$, respectively).

Although no difference was observed in the floral meristem sizes of *sup-1* and *ag-1 sup-1* at stage 3, the mutation in the *AG* gene enhanced the defect in floral meristem height in the *sup-1* mutant by stage 5 ($p = 4.2 \times 10^{-3}$; Fig. 3c, e, i, j). The introduction of the *ag* or *sup* mutations into the *clv3-2* background also further increased the floral meristem heights ($p = 6.4 \times 10^{-3}$ and $p = 1.9 \times 10^{-5}$, respectively; Fig. 3f–j). Interestingly, the phenotypic enhancement of the floral meristem widths was observed in *sup-1 clv3-2* ($p = 5.8 \times 10^{-6}$), but not in *ag-1 clv3-2* (Fig. 3i, j). In the *ag-1 sup-1 clv3-2* triple mutant, the floral meristems were taller than those of any of the parental lines (Fig. 3a–i), with a significant increase even observed between the triple mutant and *sup-1 clv3-2* ($p = 1.8 \times 10^{-3}$), which had the tallest floral meristems among the double mutants (Fig. 3g–j). These results indicate that CLV3, AG, and SUP act in partially redundant pathways and coordinately modulate the size of the floral meristem in a spatial and temporal manner. Although AG mainly functions to restrict floral meristem proliferation after stage 5, it also plays a role in the earlier stages of development, as revealed in the sensitized *sup-1* and/or *clv3-2* mutant backgrounds.

Expression of the stem cell determinant *WUS* in the mutant floral buds

To visualize the stem cell niches in the floral meristems at stage 5, we introduced the *pWUS::GFP-ER* transgene (Gordon et al. 2007) into the single, double, and triple mutant backgrounds and observed the resulting GFP signal by confocal microscopy. Wild-type floral meristems at this developmental stage showed faint *WUS* expression in their organizing center (Fig. 4a), which was repressed by stage 6 (Supplementary Fig. 1a). In *ag-1* and *sup-1* floral meristems at stage 5, *pWUS::GFP-ER* expression levels were higher than those of the wild type (Fig. 4a–c). *WUS* reporter misexpression in *clv3-2* was observed in its elongated floral meristem at stage 5 (Fig. 4d), which reflected its phenotypic abnormalities (Fletcher et al. 1999). Unlike the wild type, the *ag-1*, *sup-1*, and *clv3-2* flowers still possessed dome-shaped floral meristems even after the inner structures of the flowers were completely covered by sepals and the *WUS* reporter was expressed in their presumed organizing centers (Supplementary Fig. 1c–d).

We further investigated the *WUS* reporter expression pattern in the double and triple mutants. In the *ag-1 sup-1* double mutant at stage 5, the *WUS* expression domain was longitudinally elongated compared with its parental lines, which meant that its expression continued into the rib meristem cells (Fig. 4e). By contrast, the *WUS* expression pattern in the *ag-1 clv3-2* floral meristem was similar to that of *clv3-2* (Fig. 4d, f). The morphological changes in the floral meristem heights and widths of *sup-1 clv3-2* relative to *clv3-2* were reflected in their differences in the reporter expression domain, which was elongated in both the longitudinal and vertical directions in *sup-1 clv3-2* (Fig. 4d, g). Furthermore, the degree of GFP signal intensity in *sup-1 clv3-2* seemed higher than that of the *clv3-2* mutant. In the *ag-1 sup-1 clv3-2* triple mutant, the *pWUS::GFP-ER* expression domain and signal levels were larger and stronger than those of any other genotype (Fig. 4h). Interestingly, the reporter was never expressed in the L1 and L2 layers of stage 5 floral meristems in any of the genotypes (Fig. 4a–h, right panels).

Identification of direct targets of AG with a likely role in floral meristem development

AG mainly regulates flower size during the later stages of development. The *WUS* reporter expression domain in the *ag-1 sup-1 clv3-2* triple mutant was more than 10 times as wide as that of the *sup-1 clv3-2* double mutant at developmental stage 10 (Fig. 5a, b), which largely coincided with the mass of undifferentiated cells observed in these flowers at later stages (Fig. 1j, l).

To determine whether AG has activities in addition to repressing *WUS* expression during the termination of floral meristem activity, we performed an RNA-seq analysis using the two mutants with enlarged floral meristems (*sup-1 clv3-2* and *ag-1 sup-1 clv3-2*) as genetic tools. More than 10 M reads per sample were obtained and mapped based on TAIR10 in each sample, and the number of reads per kilobase of transcripts per million sequence reads was calculated (Supplementary Table 2). This analysis identified 2105 differentially expressed genes in total (Fig. 5c, Supplementary Table 3). Among them, 96 and 2009 genes were downregulated and upregulated in *sup-1 clv3-2*, respectively. Next, we computationally identified the AG direct targets using a published ChIP-seq dataset (Ó'Maoiléidigh et al. 2013) and found that 5% of the upregulated genes and 31% of the downregulated genes (125 in total) were bound by AG (Supplementary Table 4, Supplementary Fig. 2). To examine

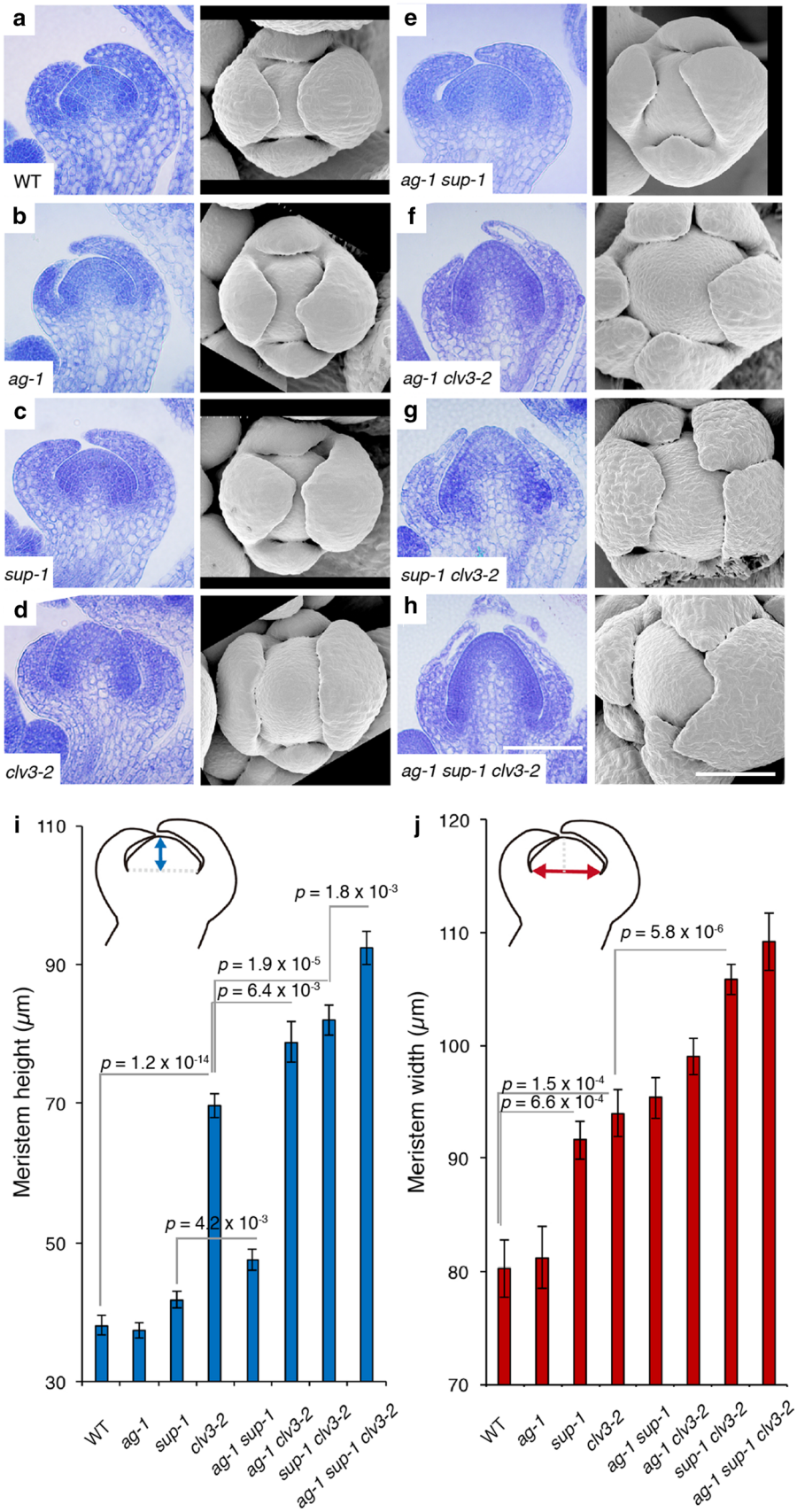

Fig. 3 Comparison of floral meristem height and width between the wild type and single, double, and triple floral buds at stage 5. **a**–**h** Side and top views of the floral buds at stage 5 formed in wild type (**a**), *ag-1* (**b**), *sup-1* (**c**), *clv3-2* (**d**), *ag-1 sup-1* (**e**), *ag-1 clv3-2* (**f**), *sup-1 clv3-2* (**g**), and *ag-1 sup-1 clv3-2* (**h**). (Left) Side views from longitudinal sections. (Right) Top views visualized using SEM. Section and SEM images are shown at the same magnification. Bar = 50 µm in **a**–**h**. **i**, **j** Quantification of floral meristem height (**i**) and width (**j**) in flowers at stage 5. Error bars represent SD of at least 13 measurements. The *p* values were calculated using a Student's *t* test

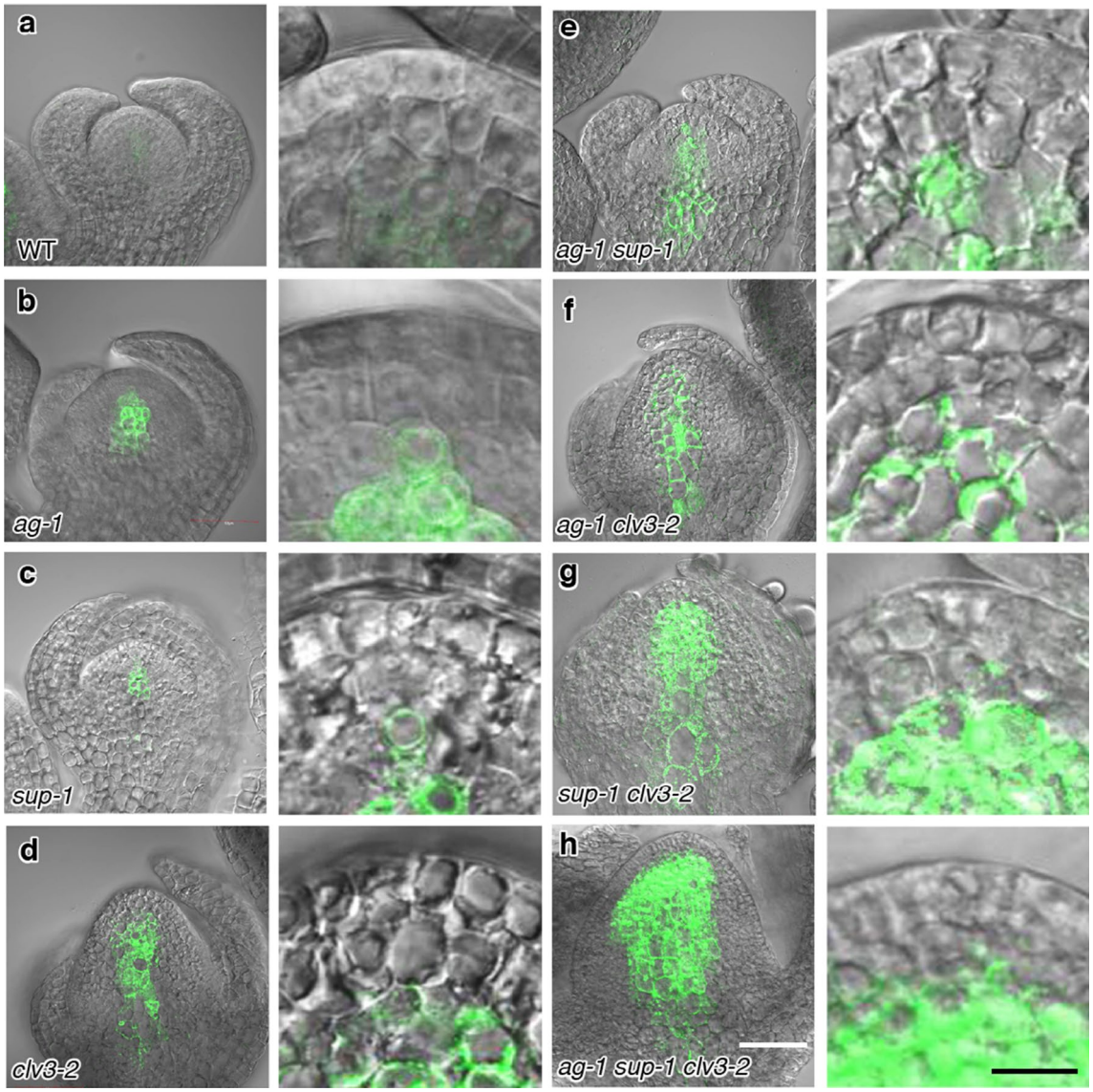

Fig. 4 Location of *WUS* expression in the wild type and single, double, and triple mutants. **a**–**h** Longitudinal sections through the *pWUS::GFP-ER* floral buds in the wild type (**a**), *ag-1* (**b**), *sup-1* (**c**), *clv3-2* (**d**), *ag-1 sup-1* (**e**), *ag-1 clv3-2* (**f**), *sup-1 clv3-2* (**g**), and *ag-1 sup-1 clv3-2* (**h**). (Left) Stage 5 floral buds. (Right) Higher magnification of floral meristems. Bar = 50 μm in **a**–**h** (left); 10 μm in **a**–**h** (right)

the likely functions of these 125 genes, we tested for GO term enrichment among them using agriGO (Fig. 5d, Supplementary Table 2; Du et al. 2010; Tian et al. 2017). We identified 85 significantly enriched GO terms (false discovery rate < 0.01; Fig. 5e, Supplementary Table 5), of which the 10 most highly enriched terms were related to either transcription or flower development (Fig. 5e). After reducing the GO terms using REVIGO (Supek et al. 2011), the enriched terms included "floral whorl development," "negative regulation of biological process," "gene expression," "reproduction," "developmental process," "multicellular organismal process," and "response to UV" (Supplementary Table 6). The GO term "floral whorl development" includes "meristem development." On the other hand, "negative regulation of biological process" includes processes that stop, prevent, or reduce the frequency, rate or extent of a biological process. Based on the REVIGO gene ontology web server (http://revigo.irb.hr/), "negative regulation of biological processes" contains 7 GO terms; "negative regulation of biological process," "regulation of cellular process," "regulation of biological process," "nucleobase-containing compound metabolic process," "RNA metabolic process," "macromolecule biosynthetic process," "regulation of transcription, DNA-templated," and "regulation of metabolic process," suggesting a negative role for AG on cellular, metabolic, or transcription process in the control of floral

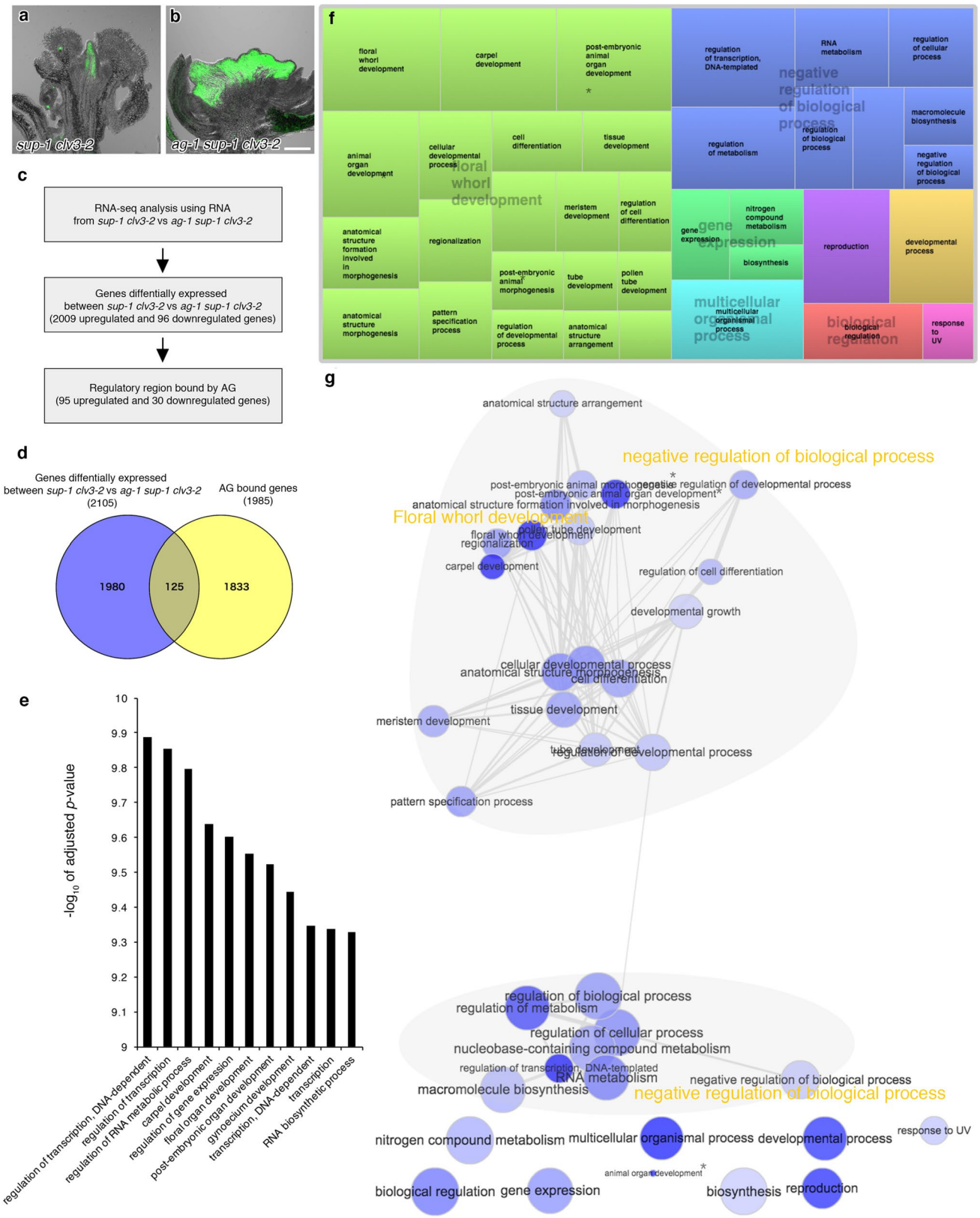
a
sup-1 clv3-2
b
ag-1 sup-1 clv3-2
c
RNA-seq analysis using RNA from sup-1 clv3-2 vs ag-1 sup-1 clv3-2
Genes diffentially expressed between sup-1 clv3-2 vs ag-1 sup-1 clv3-2 (2009 upregulated and 96 downregulated genes)
Regulatory region bound by AG (95 upregulated and 30 downregulated genes)
d
Genes diffentially expressed between sup-1 clv3-2 vs ag-1 sup-1 clv3-2 (2105)
AG bound genes (1985)
1980
125
1833
e
-log10 of adjusted p-value
10
9.9
9.8
9.7
9.6
9.5
9.4
9.3
9.2
9.1
9
regulation of transcription, DNA-dependent
regulation of transcription
regulation of RNA metabolic process
carpel development
regulation of gene expression
floral organ development
post-embryonic organ development
gynoecium development
transcription, DNA-dependent
transcription
RNA biosynthetic process
f
floral whorl development
carpel development
post-embryonic animal organ development
regulation of transcription, DNA-templated
RNA metabolism
regulation of cellular process
negative regulation of biological process
macromolecule biosynthesis
regulation of metabolism
regulation of biological process
negative regulation of biological process
animal organ development
cellular developmental process
cell differentiation
tissue development
floral whorl development
meristem development
regulation of cell differentiation
anatomical structure formation involved in morphogenesis
regionalization
gene expression
nitrogen compound metabolism
biosynthesis
reproduction
developmental process
post-embryonic animal morphogenesis
tube development
pollen tube development
anatomical structure morphogenesis
pattern specification process
regulation of developmental process
anatomical structure arrangement
multicellular organismal process
biological regulation
response to UV
g
anatomical structure arrangement
negative regulation of biological process
post-embryonic animal morphogenesis
negative regulation of developmental process
post-embryonic animal organ development
anatomical structure formation involved in morphogenesis
Floral whorl development
pollen tube development
floral whorl development
regionalization
carpel development
regulation of cell differentiation
developmental growth
cellular developmental process
anatomical structure morphogenesis
cell differentiation
tissue development
meristem development
tube development
regulation of developmental process
pattern specification process
regulation of biological process
regulation of metabolism
regulation of cellular process
nucleobase-containing compound metabolism
regulation of transcription, DNA-templated
RNA metabolism
negative regulation of biological process
macromolecule biosynthesis
negative regulation of biological process
nitrogen compound metabolism
multicellular organismal process
developmental process
response to UV
animal organ development
biological regulation
gene expression
biosynthesis
reproduction

◂**Fig. 5** Identification of direct AG targets with a likely role in floral meristems. **a**, **b** Longitudinal section through the *pWUS::GFP-ER* floral buds in *sup-1 clv3-2* (**a**) and *ag-1 sup-1 clv3-2* (**b**). **c** A flowchart of the pipeline for identifying high-confidence AG targets. Target genes are likely to be regulated in floral meristems. **d** Venn diagram showing the number of genes differentially expressed in *ag-1 sup-1 clv3-2* and *sup-1 clv3-2,* and their overlap with the direct targets of AG. **e** Gene ontology (GO) term enrichment analysis of 125 genes. The top 10 terms determined by their $-\log_{10}$-adjusted *p* values are shown. The false discovery rate (FDR) was lower than 1.0×10^{-7}. **f** The TreeMap view of GO terms. A FDR correction was conducted and a FDR cutoff of less than 0.01 was implemented. The resulting GO terms that fulfilled this criterion were further minimized using REVIGO. **g** The interactive graph view generated with REVIGO. Bright and pale colors indicate lower and higher *p* values, respectively. The size of circles indicates the frequency of the GO term in the underlying GOA database

meristems. Two major networks were visualized; the first was related to both "floral whorl development" and "negative regulation of biological process," while the second was related only to "negative regulation of biological process."

Characterization of high-confidence AG targets in floral meristems

To further characterize the 125 AG target candidate genes during flower development, we used k-means clustering and publicly available gene expression datasets. Two transcriptome datasets, one from organ initial cells and one from floral organs (Jiao and Meyerowitz 2010; Frerichs et al. 2016), were used, and two gene clusters were identified. Cluster 1 contains 30 genes that were upregulated in wild-type organ initial cells but downregulated in *sup-1 clv3-2* (thus were negatively regulated by AG; Fig. 6a, b). Real-time RT-PCR confirmed the downregulation of a selection of these genes in *sup-1 clv3-2* compared with *ag-1 sup-1 clv3-2* (Fig. 6c). This cluster contained a lot of the known regulators that promote the specification of organ initial cells and the formation of the floral meristem. Four of these genes are direct targets of auxin-dependent transcription factor MONOPTEROS (MP); *ARABIDOPSIS HISTIDINE PHOSPHOTRANSFER PROTEIN6* (*AHP6*), *TARGET OF MONOPTEROS3* (*TMO3*), *AINTEGUMENTA-LIKE6* (*AIL6*), and *LEAFY* (*LFY*) (Yamaguchi et al. 2013; Besnard et al. 2014; Wu et al. 2015). Among the 30 genes negatively regulated by AG, the expression patterns of 10 genes (Fig. 6a asterisks) were previously examined using in situ hybridization or reporter genes and were found to be expressed in organ initial cells (Blazquez et al. 1997; Byzova et al. 1999; Samach et al. 1999; Nole-Wilson and Krizek 2006; Pastore et al. 2011; Yamaguchi et al. 2013; Besnard et al. 2014; Chandler and Werr 2014; Wu et al. 2015). In cluster 1, there were no clear gene expression changes that coincided with the expression domains of *AP1, AP3,* and *AG* between stage 4 and stage 6–7 (Fig. 6a, b).

Cluster 2 contained 95 genes that were downregulated in the organ initial cells but upregulated in *sup-1 clv3* (thus activated by AG; Fig. 6a, b). This cluster contained the well-known AG-activated targets *CRABSCLAW* (*CRC*) and *SPOROCYTELESS* (*SPL*), which validated our approach (Ito et al. 2004; Gomez-Mena et al. 2005). Furthermore, real-time RT-PCR analysis confirmed that a selection of these genes were upregulated in *sup-1 clv3-2* in comparison with *ag-1 sup-1 clv3-2* (Fig. 6d). Although we observed a clear negative relationship between the gene expression in the organ initial cells and the differentially expressed genes in *sup-1 clv3-2*, none of the genes in cluster 2 have yet been linked to organ initial cell specification or floral meristem formation, unlike the genes in cluster 1. Finally, the expression levels of the meristematic marker genes *KNAT1* and *BARELY ANY MERISTEM3* (Douglas et al. 2002; Depuydt et al. 2013) were similar between *sup-1 clv3-2* and *ag-1 sup-1 clv3-2* (Fig. 6e), thus confirming the specificity of our approach. Taken together, these findings suggest that AG negatively controls the production of organ initial cells, possibly through regulating the genes identified here.

Discussion

The roles of the *AG*, *SUP*, and *CLV3* pathways in regulating floral meristem activity

Here, we revealed the genetic interactions between two flower-specific transcription factors, AG and SUP, and a secreted peptide, *CLV3*, which were originally identified using forward genetics approaches (Yanofsky et al. 1990; Clark et al. 1995; Sakai et al. 1995). Two pieces of evidence support the presence of this genetic interaction. First, phenotypic enhancement was observed when we introduced another mutation; the floral meristem of the *ag sup clv3* triple mutant is bigger than that of the wild type or any other single or double mutant (Figs. 1, 2, 3). Second, the expression domain of the key stem cell determinant marker gene *WUS* corresponded with the size of the floral meristem (Fig. 4), and the triple mutant had the largest *WUS* reporter expression domain of any mutant used in this study. Thus, we concluded that *AG*, *SUP*, and *CLV3* coordinately modulate the floral meristem activity in parallel pathways.

Although *AG* expression occurs throughout the floral meristem from stage 3 of flower development (Yanofsky et al. 1990), we did not observe an obvious difference between the wild type and the *ag-1* single mutant in terms of the floral meristem height or width by stage 5 (Figs. 2, 3; Table 1). AG was previously reported to terminate floral meristem proliferation through *WUS* repression during stage 6 of flower development (Sun and Ito 2015), which explains why we found that the *ag* mutant flower at anthesis was

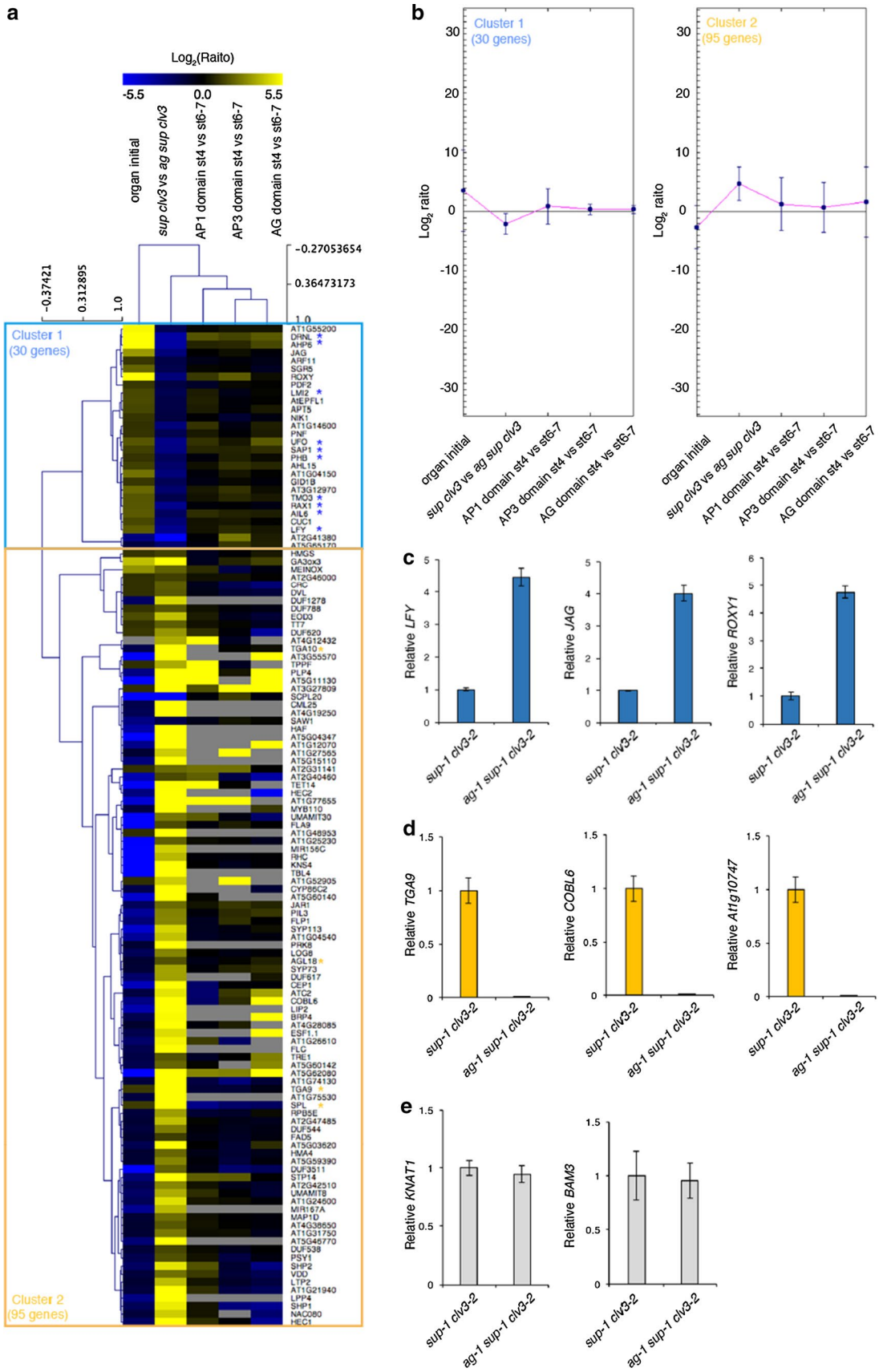
a
Log2(Raito)
-5.5
0.0
5.5
organ initial
sup clv3 vs ag sup clv3
AP1 domain st4 vs st6-7
AP3 domain st4 vs st6-7
AG domain st4 vs st6-7
-0.27053654
0.36473173
1.0
-0.37421
0.312895
1.0
Cluster 1
(30 genes)
Cluster 2
(95 genes)
b
Cluster 1
(30 genes)
Cluster 2
(95 genes)
Log2 raito
organ initial
sup clv3 vs ag sup clv3
AP1 domain st4 vs st6-7
AP3 domain st4 vs st6-7
AG domain st4 vs st6-7
c
Relative LFY
Relative JAG
Relative ROXY1
sup-1 clv3-2
ag-1 sup-1 clv3-2
d
Relative TGA9
Relative COBL6
Relative At1g10747
e
Relative KNAT1
Relative BAM3

◂**Fig. 6** Clustering of high-confidence direct AG targets in floral meristems. **a** A k-means clustering of genes directly regulated by AG. Heatmap displays the $\log_2$ expression changes of the 125 targets based on two public transcriptome datasets. Two large clusters were identified. Arrows indicate genes previously found to be expressed in floral primordia initial cells. **b** Gene expression from the two hierarchical clusters. One cluster contains 30 genes downregulated in *sup-1 clv3-2*. The other cluster contains the 95 genes upregulated in *sup-1 clv3-2*. **c**–**e** qRT-PCR verification of AG targets. Error bars represent SD of three PCR replicates of 3 biological samples. **c** Downregulated genes in *sup-1 clv3-2*. **d** Upregulated genes in *ag-1 sup-1 clv3-2*. **e** Meristem marker genes

clearly larger than that of the wild type (Fig. 1; Table 1). Thus, the *ag* mutation mainly affects the floral meristem and the resulting flower size from stage 5 onwards. Indeed, *WUS* was expressed at the center of the *ag-1* flowers even after petals were formed (Fig. 5b). Our results indicate that AG mainly controls the timing of floral meristem termination, but does not contribute much to the size of the floral meristems in the early stages of flower development, or at least its role is complemented by other genetic pathways mediated by SUP and CLV. The effects of the *ag* mutation in floral meristem height at stages 3 and 5 were seen in the sensitized *sup-1 clv3-2* double mutant background. This also supports the previous finding that AG directly binds to the *WUS* promoter and negatively regulates its expression at stages 4 and 5 (Liu et al. 2011).

The SUP protein localizes at the boundary between the incipient stamens and carpels at stage 3 (Prunet et al. 2017). In stage 5 floral buds, the *SUP* expression domain expands to a groove between the developing stamen primordia and the floral meristem (Prunet et al. 2017). Since *sup* mutants have a wider floral meristem at stage 5 than the wild type, SUP plays a role in repressing the expansion of the floral meristem along the horizontal axis (Figs. 2, 3; Table 1). We observed a morphological difference between the wild-type and *sup-1* floral buds at stage 5, but not at stage 3, suggesting that SUP inhibits floral meristem activity during stage 4 or 5. Unlike the *ag-1* mutation, the introduction of the *sup-1* mutation into a *clv3-2* or *ag-1 clv3-2* background was found to increase the height of the floral meristems even at stage 3, suggesting that SUP negatively controls the size of floral meristem from stage 3 together with AG and CLV3.

CLV3 is expressed in the stem cells of inflorescence meristems and floral meristems from stage 1 onwards (Gruel et al. 2016). As reported previously, the shape of the floral primordium in *clv3-2* is different from that of the wild type even at stage 1 of development (Szczesny et al. 2009), and floral meristems in *clv3-2* at stages 3 and 5 were wider and taller than those of the wild type (Figs. 2, 3; Table 1). Although the *clv3-2* mutant has a huge floral meristem from the early stages of flower development, its open flower is no larger than that of the wild type, and the cells located at the enlarged floral meristems appear to turn into ectopic floral organs. Interestingly, we did not see an increased flower size in *sup clv3* compared with its parental lines, demonstrating that AG prevents the enlargement of flowers in this mutant. This also indicates the presence of partially redundant pathways mediated by CLV3, SUP, and AG; both CLV3 and SUP spatially restrict the size of floral meristems, while AG mainly functions to temporally terminate floral meristem activities.

Possible roles of AG target genes in floral meristems

AG acts as a master regulator to execute its central role in the control of floral meristem activity, in large part by repressing the stem cell determinant gene *WUS* (Sun and Ito 2015). Our understanding of the precise function of floral-meristem-specific transcription factors is restricted by the very limited numbers of floral meristem cells in plants, which makes it difficult to isolate these cells without using specialized equipment such as laser microdissection or fluorescence-activated cell sorting. Our morphological analyses revealed that *ag-1 sup-1 clv3-2* had a large number of floral meristem-like cells compared with *sup-1 clv3-2* (Figs. 1, 2, 3, 4), and a total of 2105 differentially expressed genes were identified between these plants. The quantitative differences in the expression of upregulated genes in *sup-1 clv3-2* are most likely due to tissue composition for the following reasons. (1) *sup-1 clv3-2* formed more than 10 stamens per flower, while the *ag-1 sup-1 clv3-2* mutant plants did not produce any stamens. (2) *p* value of each annotation in the top 10 GO terms using upregulated genes in *sup clv3* ($p < 1.0 \times 10^{-35}$) is much lower than those using downregulated genes ($p < 1.0 \times 10^{-8}$). (3) Even though we identified more genes upregulated in *sup clv3*, only 95 out of 2009 (4.7%) are AG direct targets. By contrast, 30 out of 95 genes (31.5%) downregulated in *sup clv3* are direct targets. These tissue composition issues could affect more than the loss of transcription factor activity; genes upregulated in *sup-1 clv3-2* were involved in the later stages of flower development, mainly sporogenesis (Supplementary Fig. 3). By comparing these genes to the direct targets of AG, we narrowed down the number to 125 high-confidence AG targets likely acting in floral meristems (Fig. 5). Since a few of the known AG targets were identified using our filtering criteria (Ito et al. 2004, Gomez-Mena et al. 2005), our strategy seemed to be appropriate (Fig. 6).

A total of 35 of the 125 AG target genes are involved in transcription. This represents a significant enrichment ($p = 2.0 \times 10^{-19}$) of transcription factors in the AG target genes (28% of the AG target genes), as only 1533 (4.5%) of the 33,602 genes in the TAIR10 database encode transcription factors (Riechmann et al. 2000). We were not surprised that this list included four genes encoding MADS-box transcription factors, four homeodomain or homeodomain-like

Table 1 Summary of flower morphology the wild type and single, double, and triple mutants

Genotype	WT	*ag-1*	*sup-1*	*clv3-2*	*ag-1 sup-1*	*ag-1 clv3-2*	*sup-1 clv3-2*	*ag-1 sup-1 clv3-2*
Stage 3 FM height	+	+	+	++	+	++	+++	++++
Stage 3 FM width	+	+	+	++	+	++	++	++
Stage 6 FM height	+	+	+	+++	++	++++	++++	+++++
Stage 6 FM width	+	+	++	++	++	++	+++	+++
Stage 13 flower size	+	++	++	++	++++	+++++	+++	++++++

proteins, or four AP2-type transcription factors, since these families have important roles in flower development and/or meristem development (Ng and Yanofsky 2001; Tan and Irish 2006; Licausi et al. 2013). Although their mutant phenotypes have been characterized (Smith et al. 2004; Morita et al. 2006; Kumar et al. 2007; Hwang and Quail 2008; Magnani and Hake 2008), the roles of three homeobox genes (*SAWTOOTH*, *KNATM*, *POUND-FOOLISH*), *SHOOT GRAVITROPISM5*, and *PHYTOCHROME INTERACTING FACTOR3-LIKE1* in the termination of floral meristem activity have not yet been examined. Furthermore, *MYB DOMAIN PROTEIN110*, *AUXIN RESPONSE FACTOR11*, *REPRODUCTIVE MERISTEM11* (*REM11*) *NAC DOMAIN CONTAINING PROTEIN79*, *VERDANDI*, *At1g26610*, and *At3g57370* are largely uncharacterized.

A link between AG and "floral whorl development" was found, as expected. The functions of all 21 AG target genes involved in flower development, i.e., *PHABULOSA*, *SHATTERPROOF1* (*SHP1*), *SHP2*, *HALF FILLED*, *SPL*, *HECATE1* (*HEC1*), *HEC2*, *LFY*, *REM11*, *MIR167A*, *ROXY1*, *AGAMOUS-LIKE18* (*AGL18*), *JAGGED*, *CRC* , *CUP-SHAPED COTYLEDON1*, *GA INSENSITIVE DWARF1B*, *FLOWERING LOCUS C*, *PROTODERMAL FACTOR 2* (*PDF2*), *LMI2*, *STERILE APETALA* (*SAP*), and *AIL6,* have already been examined (Weigel et al. 1992; Aida et al. 1997; Byzova et al. 1999; Michaels and Amasino 1999; Liljegren et al. 2000; Ito et al. 2004; Ohno et al. 2004; Gomez-Mena et al. 2005; Ueguchi-Tanaka et al. 2005; Adamczyk et al. 2007; Xing and Zachgo 2008; Crawford and Yanofsky 2011; Pastore et al. 2011; Kamata et al. 2013; Rubio-Somoza and Weigel 2013; Mantegazza et al. 2014; Schuster et al. 2015; Yamaguchi et al. 2016). However, the molecular links between AG and some of those genes are not fully understood. Interestingly, while it was reported that PDF2, LFY, UNUSUAL FLORAL ORGANS (UFO), AIL6, and SAP act upstream of *AG* (Byzova et al. 1999; Chae et al. 2008; Krizek 2009; Winter et al. 2011; Kamata et al. 2013), we found that these five genes also act as downstream targets of AG. This suggests that AG is involved in a regulatory feedback mechanism, which is reasonable considering that many master regulators are regulated by their own downstream targets (Kaufmann et al. 2010).

AG is required for floral determinacy, and *ag* flowers only occasionally give rise to an inflorescence structure. Our findings, combined with previous reports and the direct and indirect *WUS* repression by AG, suggest that AG represses not only the stem cell determinant genes, but also a large set of genes specifically expressed in organ initial cells, such as *DRNL*, *AHP6*, *LFY*, *AIL6*, *TMO3*, *LMI2*, and *ROXY1* (Nag et al. 2007; Xing and Zachgo 2008; Pastore et al. 2011; Yamaguchi et al. 2013; Besnard et al. 2014; Wu et al. 2015). Four of these genes are direct targets of MP, which is key to produce floral organ founder cells. But the *MP* mRNA level was similar between *sup-1 clv3-2* and *ag-1 sup-1 clv3-2* based on RNA-seq; thus, this repression by AG is achieved without changing the transcriptional levels of *MP*. During floral meristem formation, the proper coordination of organ initial cell division is key for the creation of organ primordia. For the termination of floral meristem activity, the generation of organ initial cells around the floral meristem must be attenuated. Our expression profiling suggests that AG functions to maintain the irreversible state of reproductive development through the negative regulation of floral meristem identity genes and genes involved in organ initiation. Further studies are needed to elucidate the negative regulation of organ initial cell generation during floral meristem termination.

Acknowledgements The authors would like to thank Akie Takahashi and Taeko Kawakami for technical assistance, and Elliot Meyerowitz for providing *pWUS::GFP-ER* lines. This work was supported by Grants from Japan Science and Technology Agency "Precursory Research for Embryonic Science and Technology (No. JPMJPR15QA)," a JSPS KAKENHI (No. 16H01468), the NAIST Foundation, the Sumitomo Foundation, the Takeda Foundation, and the Mishima Kaiun Memorial Foundation to N.Y.; a Grant from JSPS KAKENHI (No. 15H05955) to T. S.; a Grant from Japan Science and Technology Agency "Precursory Research for Embryonic Science and Technology (No. JPMJPR15Q2)" to Y.I.; Grants from JSPS KAKENHI (Nos. 15H05959 and 17H06172) to K.S.; and Grants from the NAIST Foundation, the Mitsubishi Foundation, and JSPS KAKENHI (15H01234, 15H01356, 15H02405, and 17H05843) to T.I.

References

Adamczyk BJ, Lehti-Shiu MD, Fernandez DE (2007) The MADS domain factors AGL15 and AGL18 act redundantly as repressors of the floral transition in *Arabidopsis*. Plant J 50:1007–1019

Aida M, Ishida T, Fukaki H, Fujisawa H, Tasaka M (1997) Genes involved in organ separation in *Arabidopsis*: an analysis of the *cup-shaped cotyledon* mutant. Plant Cell 9:841–857

Besnard F, Refahi Y, Morin V, Marteaux B, Brunoud G, Chambrier P, Rozier F, Mirabet V, Legrand J, Laine S, Thevenon E, Farcot E, Cellier C, Das P, Bishopp A, Dumas R, Parcy F, Helariutta Y, Boudaoud A, Godin C, Traas J, Guedon Y, Vernoux T (2014) Cytokinin signaling inhibitory fields provide robustness to phyllotaxis. Nature 505:417–421

Blazquez MA, Soowal LN, Lee I, Weigel D (1997) *LEAFY* expression and flower initiation in *Arabidopsis*. Development 124:3835–3844

Bowman JL, Smyth DR, Meyerowitz EM (1989) Genes directing flower development in *Arabidopsis*. Plant Cell 1:37–52

Bowman JL, Sakai H, Jack T, Weigel D, Mayer U, Meyerowitz EM (1992) *SUPERMAN*, a regulator of floral homeotic genes in *Arabidopsis*. Development 114:599–615

Brand U, Fletcher JC, Hode M, Meyerowitz EM, Simon R (2000) Dependence of stem cell fate in *Arabidopsis* on a feedback loop regulated by *CLV3* activity. Science 289:617–619

Breuil-Broyer S, Trehin C, Morel P, Boltz V, Sun B, Chambrier P, Ito T, Negrutiu I (2016) Analysis of the *Arabidopsis* superman allelic series and the interactions with other genes demonstrate developmental robustness and joint specification of male–female boundary, flower meristem termination and carpel compartmentalization. Ann Bot 117:905–923

Byzova MV, Franken J, Aarts MG, de Almeida-Engler J, Engler G, Mariani C, Van Lookeren Campagne MM, Angenent GC (1999) *Arabidopsis STERILE APETALA*, a multifunctional gene regulating inflorescence, flower, and ovule development. Gene Dev 13:1002–1014

Chae E, Tan QK, Hill TA, Irish VF (2008) An *Arabidopsis* F-box protein acts as a transcriptional co-factor to regulate floral development. Development 135:1235–1245

Chandler JW (2011) Founder cell specification. Trends Plant Sci 16:607–613

Chandler JW, Werr W (2014) *Arabidopsis* floral phytomer development: auxin response relative to biphasic modes of organ initiation. J Exp Bot 65:3097–3110

Clark SE, Running MP, Meyerowitz EM (1995) *CLAVATA3* is a specific regulator of shoot and floral meristem development affecting the same processes as *CLAVATA1*. Development 121:2057–2067

Crawford BCW, Yanofsky MF (2011) *HALF FILLED* promotes reproductive tract development and fertilization efficiency in *Arabidopsis thaliana*. Development 138:2999–3009

Depuydt S, Rodriguez-Villalon A, Santuari L, Wyser-Rmili C, Ragni L, Hardtke CS (2013) Suppression of *Arabidopsis* protophloem differentiation and root meristem growth by CLE45 requires the receptor-like kinase BAM3. PNAS 110:7074–7079

Doerner P (2001) Plant meristems: a menage a trois to end it all. Curr Biol 11:785–787

Douglas SJ, Chuck G, Dengler RE, Pelecanda L, Riggs CD (2002) KNAT1 and ERECTA regulate inflorescence architecture in *Arabidopsis*. Plant Cell 14:547–558

Du Z, Zhou X, Ling Y, Zhang Z, Su Z (2010) agriGO: a GO analysis toolkit for the agricultural community. Nucleic Acids Res 38:W64–W70

Fletcher JC, Brand U, Running MP, Simon R, Meyerowitz EM (1999) Signaling of cell fate decisions by *CLAVATA3* in *Arabidopsis* shoot meristems. Science 283:1911–1914

Frerichs A, Thoma R, Abdallah AT, Frommolt P, Werr W, Chandler JW (2016) The founder-cell transcriptome in the *Arabidopsis* apetala1 cauliflower inflorescence meristem. BMC Genom 17:855

Gomez-Mena C, de Folter S, Costa MM, Angenent GC, Sablowski R (2005) Transcriptional program controlled by the floral homeotic gene *AGAMOUS* during early organogenesis. Development 132:429–438

Gordon SP, Heisler MG, Reddy GV, Ohno C, Das P, Meyerowitz EM (2007) Pattern formation during de novo assembly of *Arabidopsis* shoot meristem. Development 134:3539–3548

Gruel J, Landrein B, Tarr P, Schuster C, Refahi Y, Sampathkumar A, Hamant O, Meyerowitz EM, Jonsson H (2016) An epidermis-driven mechanism positions and scales stem cell niches in plants. Sci Adv 2:e1500989

Hwang YS, Quail PH (2008) Phytochrome-regulated PIL1 derepression is developmentally modulated. Plant Cell Physiol 49:501–511

Ikeda M, Mitsuba N, Ohme-Takagi M (2009) *Arabidopsis* WUSCHEL is a bifunctional transcription factor that acts as a repressor in stem cell regulation and as an activator in floral patterning. Plant Cell 21:3493–3505

Ito T, Sakai H, Meyerowitz EM (2003) Whorl-specific expression of the *SUPERMAN* gene of *Arabidopsis* is mediated by *cis* elements in the transcribed region. Curr Biol 13:1524–1530

Ito T, Wellmer F, Yu H, Das P, Ito N, Alves-Ferrelra M, Rlechmann JL, Meyerowitz EM (2004) The homeotic protein AGAMOUS controls microsporogenesis by regulation of *SPOROCYTELESS*. Nature 430:356–360

Ito T, Ng KH, Lim TS, Yu H, Meyerowitz EM (2007) The homeotic protein AGAMOUS controls late stamen development by regulating a jasmonate biosynthetic gene in *Arabidopsis*. Plant Cell 19:3516–3529

Jiao Y, Meyerowitz EM (2010) Cell-type specific analysis of translating RNAs in developing flowers reveals new levels new levels of control. Mol Syst Biol 6:419

Kamata N, Okada H, Komeda Y, Takahashi T (2013) Mutations in epidermis-specific HD-ZIP IV genes affect floral organ identity in *Arabidopsis thaliana*. Plant J 75:430–440

Kaufmann K, Pajoro A, Angenent GC (2010) Regulation of transcription in plants: mechanisms controlling developmental switches. Nat Rev Genet 11:830–842

Kieffer M, Stern Y, Cook H, Clerici E, Maulbetsch C, Laux T, Davies B (2006) Analysis of the transcription factor WUSCHEL and its functional homologue in *Antirrhinum* reveals a potential mechanism for their roles in meristem maintenance. Plant Cell 18:560–573

Kondo T, Sawa S, Kinoshita A, Mizuno S, Kakimoto T, Fukuda H, Sakagami Y (2006) A plant peptide encoded by *CLV3* identified by in situ MALDI-TOF MS analysis. Science 313:845–848

Krizek BA (2009) *AINTEGUMENTA* and *AINTEGUMENTA-LIKE6* act redundantly to regulate *Arabidopsis* floral growth and patterning. Plant Physiol 150:1916–1929

Kumar R, Kushalappa K, Godt D, Pidkowich MS, Pastorelli S, Hepworth SR, Haughn GW (2007) The *Arabidopsis* BEL1-LIKE HOMEODOMAIN Protein SAW1 and SAW2 act redundantly to regulate KNOX expression spatially in leat margins. Plant Cell 19:2719–2735

Laux T, Mayer KF, Berger J, Jurgens G (1996) The *WUSCHEL* gene is required for shoot and floral meristem integrity in *Arabidopsis*. Development 122:87–96

Lenhard M, Bohnert A, Jurgens G, Laux T (2001) Termination of stem cell maintenance in *Arabidopsis* floral meristems by interactions between *WUSCHEL* and *AGAMOUS*. Cell 105:805–814

Licausi F, Ohme-Takagi M, Perata P (2013) APETALA2/ethylene responsive factor (AP2/ERF) transcription factors: mediators of stress responses and developmental programs. New Phytol 199:639–649

Liljegren SJ, Ditta GS, Eshed Y, Savidge B, Bowman JL, Yanofsky MF (2000) *SHATTERPROOF* MADS-box genes controls dispersal in *Arabidopsis*. Nature 404:766–770

Liu X, Kim YJ, Muller R, Yumul RE, Liu C, Pan Y, Cao X, Goodrich J, Chen X (2011) *AGAMOUS* terminates floral stem cell maintenance in *Arabidopsis* by directly repressing *WUSCHEL* through recruitment of polycomb group proteins. Plant Cell 23:3654–3670

Lohmann JU, Hong RL, Hode M, Busch MA, Parcy F, Simon R, Weigel D (2001) A molecular link between stem cell regulation and floral patterning in *Arabidopsis*. Cell 105:793–803

Magnani E, Hake S (2008) *KNOX* lost the *OX*: the *Arabidopsis* KNATM gene defines a novel class of KNOX transcriptional regulators missing the homeodomain. Plant Cell 20:875–887

Mantegazza O, Gregis V, Mendes MA, Morandini P, Alves-Ferreira M, Patreze CM, Nardeli SM, Kater MM, Colombo L (2014) Analysis of the *Arabidopsis* REM gene family predicts functions during flower development. Ann Bot 114:1507–1515

Mayer KF, Schoof H, Haecker A, Lenhard M, Jurgens G, Laux T (1998) Role of *WUSCHEL* in regulating stem cell fate in the *Arabidopsis* shoot meristem. Cell 95:805–815

Meyerowitz EM (1997) Control of cell division patterns in developing shoots and flowers of *Arabidopsis thaliana*. Cold Spring Harb Symp Quant Biol 62:369–375

Michaels SD, Amasino RM (1999) *FLOWERING LOCUS C* encodes a novel MADS domain protein that acts as a repressor of flowering. Plant Cell 11:949–956

Morita MT, Sakaguchi K, Kiyose S, Taira K, Kato K, Nakamura M, Tasaka M (2006) A C_2H_2-type zinc finger protein, SGR5, is involved in early events of gravitropism in *Arabidopsis* inflorescence stems. Plant J 47:619–628

Nag A, Yang Y, Jack T (2007) *DORNROSCHEN-LIKE*, an AP2 gene, is necessary for stamen emergence in *Arabidopsis*. Plant Mol Biol 65:219–232

Ng M, Yanofsky MF (2001) Function and evolution of the plant MADS-box gene family. Nat Rev Genet 2:186–195

Nole-Wilson S, Krizek BA (2006) *AINTEGUMENTA* contributes to organ polarity and regulates growth of lateral organs in combination with *YABBY* genes. Plant Physiol 141:977–987

Ó'Maoiléidigh DS, Wuest SE, Rae L, Raganelli A, Ryan PT, Kwasniewska K, Das P, Lohan AJ, Loftus B, Graciet E, Wellmer F (2013) Control of reproductive floral organ identity specification in *Arabidopsis* by the C function regulator AGAMOUS. Plant Cell 25:2482–2503

Ogawa M, Shinohara H, Sakagami Y, Matsubayashi Y (2008) *Arabidopsis* CLV3 peptide directly binds CLV1 ectodomain. Science 319:294

Ohno CK, Reddy GV, Heisler MG, Meyerowitz EM (2004) The *Arabidopsis JAGGED* gene encodes a zinc finger protein that promotes leaf tissue development. Development 131:1111–1122

Okamuro JK, de Boer BGW, Lotys-Prass C, Szeto W, Jofuku KD (1996) Flowers into shoots: photo and hormonal control of a meristem identity switch in *Arabidopsis*. PNAS 93:13831–13836

Pastore JJ, Limpuangthip Yamaguchi Y, Wu MF, Sang Y, Han SK, Malaspina L, Chavdaroff N, Yamaguchi A, Wagner D (2011) LATE MERISTEM IDENTITY2 acts together with LEAFY to activate *APETALA1*. Development 138:3189–3198

Perales M, Rodriguez K, Snipes S, Yadav RK, Diaz-Mendoza Reddy GV (2016) Threshold-dependent transcriptional discrimination underlies stem cell homeostasis. PNAS 113:6298–6306

Prunet N, Yang W, Das P, Meyerowitz EM, Jack TP (2017) *SUPERMAN* prevents class B gene expression and promotes stem cell termination in the fourth whorl of *Arabidopsis thaliana* flowers. PNAS 114:7166–7171

Riechmann JL, Heard J, Martin G, Reuber L, Jiang C, Keddie J, Adam L, Pineda O, Ratcliffe OJ, Samaha RR, Creelman R, Pilgrim M, Broun P, Zhang JZ, Ghandehari D, Sherman BK, Yu G (2000) *Arabidopsis* transcription factors: genome-wide comparative analysis among eukaryotes. Science 290:2105–2110

Rodriguez K, Perales M, Snipes S, Yadav RK, Diaz-Mendoza M, Reddy GV (2016) DNA-dependent homodimerization, sub-cellular partitioning, and protein destabilization control WUSCHEL levels and spatial patterning. PNAS 113:6307–6315

Rubio-Somoza I, Weigel D (2013) Coordination of flower maturation by a regulatory circuit of three microRNAs. PLoS Genet 9:e1003374

Sakai H, Medrano LJ, Meyerowitz EM (1995) Role of *SUPERMAN* in maintaining *Arabidopsis* floral whorl boundaries. Nature 378:199–203

Samach A, Klenz JE, Kohalmi SE, Risseeuw E, Haughn GW, Crosby WL (1999) The *UNUSUAL FLORAL ORGANS* gene of *Arabidopsis thaliana* is an F-box protein required for normal patterning and growth in the floral meristem. Plant J 20:433–445

Sawa S, Ito T, Shimura Y, Okada K (1999) *FILAMENTOUS FLOWER* Controls the formation and development of *Arabidopsis* inflorescences and floral meristems. Plant Cell 11:69–86

Schoof H, Lenhard M, Haecker A, Mayer KF, Jurgens G, Laux T (2000) The stem population of *Arabidopsis* shoot meristem is maintained by a regulatory loop between the *CLAVATA* and *WUSCHEL* genes. Cell 100:635–644

Schuster C, Gaillochet C, Lohmann JU (2015) *Arabidopsis* HECATE genes function in phytohormone control during gynoecium development. Development 142:3343–3350

Smith HMS, Campbell BC, Hake S (2004) Competence to respond to floral inductive signals requires the homeobox genes *PENNYWISE* and *POUND-FOOLISH*. Curr Biol 14:812–817

Smyth DR, Bowman JL, Meyerowitz EM (1990) Early flower development in *Arabidopsis*. Plant Cell 2:755–767

Sun B, Ito T (2015) Regulation of floral stem cell termination. Front Plant Sci 6:17

Sun B, Xu Y, Ng KH, Ito T (2009) A timing mechanism for stem cell maintenance and differentiation in the *Arabidopsis* floral meristem. Gene Dev 23:1791–1804

Sun B, Looi LS, Guo S, He Z, Gan ES, Huang J, Xu Y, Wee WY, Ito T (2014) Timing mechanism dependent on cell division is invoked by polycomb eviction in plant stem cells. Science 343:498–499

Supek F, Bosnjak M, Skunca N, Smuc T (2011) REVIGO summarizes and visualizes long lists of Gene Ontology terms. PLoS ONE 6:e21800

Szczesny T, Routier-Kierzkowska AL, Kwiatkowska D (2009) Influence of *clavata3-2* mutation on early flower development in *Arabidopsis thaliana*: quantitative analysts of changing geometry. J Exp Bot 60:679–695

Szemenyei H, Hannon M, Long JA (2008) TOPLESS mediates auxin-dependent transcriptional repression during *Arabidopsis* embryogenesis. Science 319:1384–1386

Tan QK, Irish VF (2006) The *Arabidopsis* zinc finger-homeodomain genes encode proteins with unique biochemical properties that are coordinately expressed during floral development. Plant Physiol 140:1095–1108

Tian T, Liu Y, Yan H, You Q, Yi X, Du Z, Xu W, Su Z (2017) agriGO v2.0: a GO analysis toolkit for the agricultural community, 2017 update. Nucleic Acids Res 45:W122–W129

Townsley BT, Covington MF, Ichihashi Y, Zumstein K, Sinha NR (2015) Brad-seq: breath adapter directional sequencing: a streamlined, ultra-simple and fast library preparation and fast library preparation protocol for strand specific mRNA library construction. Front Plant Sci 6:366

Ueguchi-Tanaka M, Ashikari M, Nakajima M, Itoh H, Katoh E, Kobayashi M, Chow TY, Hsing YI, Kitano H, Yamaguchi I, Matsuoka M (2005) GIBBERELLIN INSENSITIVE DWARF1 encodes a soluble receptor for gibberellin. Nature 437:693–698

Weigel D, Alvarez J, Smyth DR, Yanofsky MF, Meyerowitz EM (1992) *LEAFY* controls floral meristem identity in *Arabidopsis*. Cell 69:843–859

Winter CM, Austin RS, Blanvillain-Baufume S, Reback MA, Monniaux M, Wu MF, Sang Y, Yamaguchi A, Yamaguchi N, Parker JE, Parcy F, Jensen ST, Li H, Wagner D (2011) LEAFY target genes reveal floral regulatory logic, *cis* motifs, and a link to biotic stimulus response. Dev Cell 20:430–443

Winter CM, Yamaguchi N, Wu MF, Wagner D (2015) Transcriptional programs regulated by LEAFY and APETALA1 at the time of flower formation. Physiol Plant 155:55–73

Wu MF, Yamaguchi N, Xiao J, Bargmann B, Estelle M, Sang Y, Wagner D (2015) Auxin-regulated chromatin switch directs acquisition of flower primordium founder fate. eLife 4:e09269

Xing S, Zachgo S (2008) ROXY1 and ROXY2, two *Arabidopsis* glutaredoxin genes, are required for anther development. Plant J 53:790–801

Yamaguchi N, Komeda Y (2013) The role of CORYMBOSA1/BIG and auxin in the growth of *Arabidopsis* pedicel and internode. Plant Sci 209:64–74

Yamaguchi N, Wu MF, Winter CM, Berns MC, Nole-Wilson S, Yamaguchi A, Coupland G, Krizek B, Wagner D (2013) A molecular framework for auxin-mediated initiation of flower primordia. Dev Cell 24:271–282

Yamaguchi N, Winter CM, Wu MF, Kanno Y, Yamaguchi A, Seo M, Wagner D (2014) Gibberellin acts positively then negatively to control onset of flower formation in *Arabidopsis*. Science 344:638–641

Yamaguchi N, Jeong CW, Nole-Wilson S, Krizek BA, Wagner D (2016) AINTEGUMENTA and AINTEGUMENTA-LIKE6/PLETHORA3 Induce *LEAFY* Expression in Response to Auxin to Promote the Onset of Flower Formation in *Arabidopsis*. Plant Physiol 170:283–293

Yamaguchi N, Huang J, Xu Y, Tanoi K, Ito T (2017) Fine-tuning of auxin homeostasis governs the transition from floral stem cell maintenance to gynoecium formation. Nat Commun 8:1125

Yanofsky MF, Ma H, Bowman JL, Drews GN, Feldmann KA, Meyerowitz EM (1990) The protein encoded by the *Arabidopsis* homeotic gene *agamous* resembles transcription factors. Nature 346:35–39

Zhou Y, Liu X, Engstrom EM, Nimchuk ZL, Pruneda-Paz JL, Tarr PT, Yan A, Kay SA, Meyerowitz EM (2015) Control of plant stem cell function by conserved interacting transcriptional regulators. Nature 547:377–380